



University of Warwick institutional repository: <http://go.warwick.ac.uk/wrap>

This paper is made available online in accordance with publisher policies. Please scroll down to view the document itself. Please refer to the repository record for this item and our policy information available from the repository home page for further information.

To see the final version of this paper please visit the publisher's website. Access to the published version may require a subscription.

Author(s): Dawid Toton, Christian D Lorenz, Nikolaos Rompotis, Natalia Martsinovich and Lev Kantorovich

Article Title: Temperature control in molecular dynamic simulations of non-equilibrium processes

Year of publication: 2010

Link to published article:

<http://dx.doi.org/10.1088/0953-8984/22/7/074205>

Publisher statement: None

# Temperature Control in Molecular Dynamic Simulations of Non-Equilibrium Processes

Dawid Toton<sup>†</sup>, Christian D. Lorenz<sup>‡</sup>, Nicolas Rompotis<sup>††</sup>, Natalia Martsinovich<sup>#</sup> and Lev Kantorovich

October 19, 2009

Physics, King's College London, The Strand, London, WC2R 2LS, United Kingdom

<sup>†</sup>Dept. of Physics of Nanostructures and Nanotechnology, Institute of Physics, Jagiellonian University, Reymonta, Krakow, 4 PL 30-059, Poland

<sup>‡</sup>Materials Research Group, Division of Engineering, King's College London, The Strand, London, WC2R 2LS, United Kingdom

<sup>††</sup>Imperial College, High Energy Physics Department, Blackett Laboratory, Prince Consort Road, London SW7 2BW, United Kingdom

<sup>#</sup>Department of Chemistry University of Warwick Coventry CV4 7AL United Kingdom

## Abstract

Thermostats are often used in various condensed matter problems, e.g. when a biological molecule undergoes a transformation in a solution, a crystal surface is irradiated with energetic particles, a crack propagates in a solid upon applied stress, two surfaces slide with respect to each other, an excited local phonon dissipates its energy into a crystal bulk, and so on. In all these problems, as well as in many others, there is an energy transfer between different local parts of the entire system kept at a constant temperature. Very often, when modeling such processes using Molecular Dynamics (MD) simulations, thermostatting is done using strictly equilibrium approaches served to describe the NVT ensemble. In this paper we critically discuss the applicability of such approaches to *non-equilibrium* problems, including those mentioned above, and stress that the correct temperature control can only be achieved if the method is based on the Generalised Langevin Equation (GLE). Specifically, we emphasize that a meaningful compromise between computational efficiency and a physically appropriate implementation of the NVT thermostat can be achieved, at least for solid state and surface problems, if the so-called Stochastic Boundary Conditions (SBC), recently derived from the GLE [L. Kantorovich and N. Rompotis - Phys. Rev. B**78**, 094305 (2008)], are used. In SBC, the Langevin thermostat is only applied to the outer part of the simulated fragment of the entire system which borders the surrounding environment (not considered explicitly) serving as a heat bath. This point is illustrated by comparing the performance of the SBC and some of the equilibrium thermostats in two problems: (i) irradiation of the Si(001) surface with an energetic CaF<sub>2</sub> molecule using an *ab initio* Density Functional Theory (DFT) based method, and (ii) the tribology of two amorphous SiO<sub>2</sub> surfaces coated by self-assembled monolayers of methyl-terminated hydrocarbon alkoxy-silane molecules using a classical atomistic force field. We discuss the differences in the behaviour of these systems due to applied thermostatting, and show that in some cases a qualitatively different physical behaviour of the simulated system can be obtained if an equilibrium thermostat is used.

## 1 Introduction

Molecular Dynamics (MD) simulations have become a powerful tool in studying both equilibrium and non-equilibrium atomistic processes in condensed matter [1]. The microcanonical NVE ensemble in which the number of particles  $N$ , the volume  $V$ , and the total energy  $E$ , are conserved, can be generated by simply running Newtonian equations of motions for the atoms in the system. This ensemble can only be used for isolated systems. If a system at constant temperature  $T$  is to be modeled, then the NVT ensemble must be generated instead, so that the system trajectory would visit regions in the phase space according to the canonical distribution.

The simplest and the earliest approach (which is still being used) is to re-scale the atomic velocities to force the system to be at the required temperature. This method is not able to generate the canonical distribution since the kinetic energy of particles actually fluctuates in the canonical ensemble. In another rather popular proposal due to Berendsen [2] the equations of motion of atoms are supplemented by an artificial "equation of motion" for the total

kinetic energy which drives it to the correct value corresponding to the preset temperature. Again, the canonical distribution is not generated in this case.

At present, a number of prescriptions exist to ensure that the system is evolved in time according to the canonical ensemble. In the Andersen thermostat [3], a particle chosen at random is given a velocity extracted from the Maxwell distribution; this corresponds to a Markov's chain whose probability density at long times converges to the canonical distribution. In the Nosé thermostat [4, 5] (an equivalent form was suggested by Hoover [6]), an extra degree of freedom is introduced and the system evolves according to the microcanonical distribution in the extended phase space; at the same time, in the actual phase space the distribution is exactly canonical. If the Nosé thermostat is deterministic, the Andersen thermostat is stochastic and leads to non-smooth trajectories. Another popular stochastic thermostat which also generates the correct canonical distribution is the Langevin thermostat [7] (see also [8]). In this thermostat, friction forces and Gaussian distributed random forces are added to each atom of the system replacing the actual Newtonian equations of motion with stochastic differential equations (SDE); the friction forces remove energy from the simulated portion of the system, while the random forces add energy, resulting in an efficient control of the system temperature. This thermostat generates the canonical distribution since it is the stationary solution of the Fokker-Plank equation which corresponds to the Langevin SDEs. Recently, a new stochastic thermostat has been proposed [9] based on velocity rescaling by a common random factor. To obtain this factor, the evolution equation for the kinetic energy of the Berendsen thermostat is effectively replaced with a SDE for the kinetic energy. This algorithm also guarantees the correct sampling of the canonical distribution. Finally, stochastic algorithms based on random collisions of the system particles with those in the heat bath has been proposed in [10, 11, 12]. A deterministic algorithm also based on collisions with thermal bath walls was proposed in [13]. A discussion of some temperature control methods for thermal conduction problems is given in [14].

All of the thermostats mentioned above are NVT thermostats and describe systems strictly in *thermodynamic equilibrium*. Nevertheless, they are widely used for *non-equilibrium* phenomenon as the following, rather arbitrary, selection of examples illustrates.

Our first set of examples is related to tribology when MD simulations are run to calculate the friction force between two surfaces sliding with respect to each other. Two implementations can be found in the literature: when a thermostat is applied to all atoms of the system, or when only some specific atoms are thermostated. In the latter case, the chosen atoms would normally belong to several layers at the bottom of the substrate and the top of the upper sliding surface, next to the fixed layers served to mimic the missing bulk of the two surfaces. References [15, 16, 17, 18, 19, 20, 21] correspond to the first group, where we can see examples of velocity rescaling [17, 18, 19, 21], Berendsen [15, 20] and Nosé [16] thermostats used. The outer parts of the system (i.e. the second group) were thermostated with the Berendsen thermostat in [22], while the Langevin thermostat was applied in [23, 24, 25, 26].

Next we shall consider the impact (or irradiation) problems when a particle with a considerable kinetic energy hits a surface of a crystal. Similar to the above examples, all system atoms are thermostated in [27, 28] with an unspecified NVT thermostat, while in other studies either Berendsen [29, 30, 31], velocity rescaling [32] or Langevin [33, 34] thermostats are applied only to the border atoms of the cell.

Examples like these can easily be continued by presenting MD studies from other areas of materials science. For instance, in [35], a propagation of a crack in silicon due to applied tensile load was simulated using an MD technique with the Langevin thermostat applied to all atoms in the system to sample the canonical distribution [36]. In the study of the lifetimes of defect-related local phonons in the bulk silicon [37] MD simulations in the NVE ensemble were used to study the relaxation of the excited local phonons. In biological applications, e.g. when considering protein folding in a solution, Berendsen, Langevin or Nosé thermostats applied to all atoms of the system are frequently used (see e.g. a discussion in [38]), although it is argued that the Langevin thermostat is "better" due to "a more uniform distribution" of temperature throughout the protein-solution system. In [39] Berendsen and Langevin thermostats are applied to the same problem, however, the authors discuss two conflicting models of their application: whether all atoms or only the solvent atoms are thermostated. The application of the thermostat to only the solvent atoms is advocated in the paper as a more physically sound method to represent the energy transfer through the solvent. In studying energy dissipation in Atomic Force Microscopy (AFM), where an atomically sharp tip comes in contact with a surface during its oscillations [40, 41], a Langevin thermostat was applied to atoms at the top of the tip and at the bottom of the surface, similarly to some of the tribology models mentioned above. Finally, the Langevin thermostat was also applied [42] to model surface chemical reactions (e.g. chemisorption and dissociation) and solvents [43].

In some of the examples above the friction and random forces were only added to the outer part of the system which borders the missing environment region. It was suggested in [44] that the method of this kind, named

Stochastic Boundary Conditions (SBC), should be useful in studying various localized processes in condensed media. However, no formal proof of this proposal was presented then; it was only hinted much later in [41] that SBC may be derived from the Generalised Langevin Equation (GLE) (see below), but no formal proof was given.

One can see from the examples given above that the choice of one or the other method (i.e. which particular thermostat to use and whether it is to be applied to all or only to some selected atoms) is mostly decided on the grounds of practical applicability or convenience. In some cases intuitive physical arguments are also given, especially concerning the way the particular thermostat is applied (e.g. only to atoms at the system boundary). Of course, on physical grounds alone any thermostat is perfectly suitable if one is interested in *equilibrium* properties (e.g. phonon density of states of a bulk crystal or a radial distribution function in a liquid), as long as the algorithm applied samples system trajectories from the canonical distribution corresponding to the desired temperature  $T$ .

This is however not true in all the examples mentioned above since the systems studied there were *not* at thermodynamic equilibrium. Indeed, in some tribological simulations two surfaces slide with respect to each other (with a possible liquid or collection of molecules serving as a lubricant between them [21, 19]), and during this process substantial distortion happens in the junction, even bonds may be formed and broken with substantial consumption and/or release of energy. This energy is either taken from or dissipated to the environment which is maintained at a given  $T$  and located above and below the upper and lower surfaces. A similar situation is in other cases, e.g. in fracture propagation, irradiation problems, relaxation of local phonons and protein folding. In all cases an NVT simulation implies that the actual simulation system is surrounded by a heat bath kept at a given temperature; the bath is so large that any energy taken from or dissipated into it will be much smaller than its total energy, and hence will not affect its temperature.

It is important to realize that the energy of the simulated system is governed *only* via its exchange with the thermostat (the heat bath), so that controlling the temperature by applying any of the thermostats to *all atoms* of the simulated system is physically incorrect. As a result, the atomic trajectories are also incorrect since they are influenced by the thermostat applied. This artificial equilibration may have undesired physical consequences which may lead to incorrect description of the process at hand. For instance, e.g. during irradiation process, the enforced temperature control on all atoms may result in the projectile and the surrounding region being cooled down much faster than it should and this will have an effect on the structure of the track the projectile creates in the crystal, especially at longer times when the local temperature is roughly of the same order as the energy barriers corresponding to the defect formation. Moreover, all of the equilibrium thermostats have some parameters which can be tweaked to control the equilibration rate; however, these are artificial and are not related to any physical relaxation times, so that choosing particular values for these may result in artificial time dependence.

The situation is similar to using Metropolis Monte Carlo (MC) algorithm to a time-dependent problem: the equilibrium MC is strictly applicable to only sampling the canonical distribution in the phase space, it does not provide the actual *time evolution* of the system since the system trajectory in the phase space will have no physical significance. If the calculation of the actual trajectory is desired, the Kinetic Monte Carlo (KMC) algorithm must be used (see [45] and references therein).

Intuitively, a much more appealing method is the one where only boundary atoms of the system coming into contact with the environment (not treated explicitly in the simulations), are thermostated [22, 29, 30, 31, 32, 33, 34, 39, 40]. Indeed, the thermostated atoms in this method serve to mimic the “missing” environment of the entire system which, one may assume, is kept at thermodynamic equilibrium and is thus canonical. The problem is that the size of this subsystem, atoms of which are subjected to one of the thermostats (and hence which equations of motion are modified), is usually much smaller than the size of the “central region”, atoms of which move due to usual Newtonian’s equations of motion containing “natural” forces due to interatomic interactions only. Therefore, results of the simulations would depend on the particular thermostat being used.

Of course, a straightforward *numerical* solution of this problem would be to use a much bigger thermostated border region explicitly in the simulations [14]. However, this method would be completely impractical. Mori and Zwanzig [46, 47, 48] gave an elegant, albeit formal, general solution to this problem by showing that it can be recast into a form of a Generalised Langevin Equation (GLE) which takes complete and rigorous care of the environment region surrounding the “central region” (also called the “primary zone”), i.e. the actual simulation box. The GLE method has been later extended by other authors [49, 50, 51, 52, 53, 54, 55, 56, 57, 58, 59, 60, 61, 62, 63]. Basically, it has been shown that the effect of the environment, not explicitly represented in MD simulations which are run on a final subsystem of an extended system, can be included by adding random and friction forces (with memory) to *every* atom in the simulation box. The environment is assumed to be at *thermodynamic equilibrium* and described by the corresponding canonical distribution at temperature  $T$ . Then, it is shown that the random forces acting on atoms are Gaussian distributed and their autocorrelation function is proportional to the kernel in the friction memory term (which is one of the manifestations of the 2nd fluctuation-dissipation theorem) [54, 55, 48, 62].

In the special and important case of the *harmonic* environment region(s), the random force and the friction kernel of the GLE can be worked out further [54, 55, 62]. Specifically, it was shown [62] that the friction kernel as well as the dispersion of the random force can directly be related to the phonon Green’s function of the environment region (see also [59, 61, 64]). We also note that in this case the GLE explicitly contains an additional force acting on atoms in the “central region” due to an elastic response of the environment to their movement [62]; this response is essential in e.g. irradiation and fracture propagation simulations when a large energy is released in the simulated “central region” results in an elastic wave propagating out of the region towards the border of the simulation box. If the elastic response of the environment is not implemented, the elastic wave would eventually (in fact, quite quickly in simulations involving relatively small “central regions”) get reflected from the boundary putting a natural limit on the duration of the meaningful MD simulation. Next, it was also proven in [62] that after some time the finite “central region” arrives at thermodynamic equilibrium described by the canonical distribution at the same temperature  $T$  as that of the environment, and with an effective Hamiltonian which incorporates the elastic energy of the environment.

Although it is possible, at least in principle, to obtain both the friction kernel and the distribution of the random force necessary to run the GLE-based MD simulations as explained above, the final procedure is still rather complicated. Firstly, it is still extremely time consuming and, secondly, it requires knowledge of the phonon Green’s function of the system(s) representing the environment and the latter usually has a complex shape with no periodic symmetry. Therefore, the full implementation of this method, as far as we are aware, does not yet exist.

At the same time, it was recently shown in [63] that under an assumption of *short-range* interaction between atoms, the exact GLE can be recast into a form in which the elastic, friction and random forces are only added to atoms which are at the boundary of the simulation region, i.e. to the atoms which border the environment region(s); atoms belonging to the “inner region” experience only direct interatomic forces due to surrounding atoms, i.e. for these atoms the equations of motion are Newtonian, i.e.  $m_i\ddot{r}_i = F_i$ , where  $F_i$  is the total force due to all atoms in the simulation box acting on the  $i$ -th degree of freedom  $r_i$ , with  $m_i$  being the corresponding mass. Further, it was also shown that if one assumes that the random forces on different atoms are not correlated, the elastic force due to environment is negligible and that one can neglect the memory effects (i.e. that the correlation functions of the random forces decay much faster than the relevant simulation time), then the GLEs for the border atoms take exactly the Langevin form:

$$\dot{p}_i = F_i - \gamma_i p_i + f_i \quad (1)$$

where  $i$  corresponds to the degrees of freedom of the border atoms only,  $p_i = m_i\dot{r}_i$  being the corresponding momentum. Furthermore, for each degree of freedom  $i$ , the Gaussian distribution function of the random force  $f_i$  has the dispersion  $\sigma_i$  which is related directly to the friction coefficient  $\gamma_i$  in the friction force above via the well-known expression  $\sigma_i^2 = 2m_i\gamma_ik_B T/\tau$  [1], where  $k_B$  is the Boltzmann constant and  $\tau$  is the MD time step. Finally, it was proven that this relationship between the dispersion of the random force and the corresponding friction coefficient guarantees that the system will arrive at thermodynamic equilibrium described by the canonical distribution of temperature  $T$ . This is an interesting finding in its own right: even though the Langevin thermostat is applied to a subset of atoms in the simulated system (the border atoms), it can still be used for the equilibration as the correct NVT thermostat, i.e. the atomic trajectories will sample the canonical distribution. One can easily see that this method is nothing but the SBC method to which a number of authors arrived intuitively, as mentioned above. An important point is that the SBC approach has found its justification as the method of choice for non-equilibrium MD simulations. Indeed, on the one hand, it follows from the exact method based on the GLE; on the other hand, in spite of the approximations made to make it computationally accessible, it serves as the correct thermostat, i.e. guarantees the system to arrive at the appropriate canonical distribution. This means that the SBC method should be able to describe correctly the approach of the initially non-equilibrium system to equilibrium. Therefore, from all the methods mentioned above to control the temperature during a non-equilibrium process, only the SBC based on the Langevin thermostat applied to only the border atoms appears to be the correct technique which is both computationally efficient and physically appealing.

The purpose of this paper is twofold. Firstly, we shall discuss in detail our particular implementation of the SBC method. We have implemented it in the classical SciFi [65] and LAMMPS [66] codes, as well as in the *ab initio* Density Functional Theory (DFT) SIESTA code [67]. Secondly and most importantly, we provide numerical illustrations of the points made above. Namely, we consider some non-equilibrium processes using the SBC and one of the conventional equilibrium methods of thermostatting to discuss differences in the systems behaviour in the two cases. We hope that this study will help to clarify the importance of using the appropriate thermostat in running MD simulations of processes which are accompanied by an energy redistribution within a large system.

The paper is organised as follows. In the next Section we shall consider our SBC implementation for the silicon which goes along similar lines to that in [41, 40]. In Section 3 an energetic  $\text{CaF}_2$  molecule incident on the Si(001)

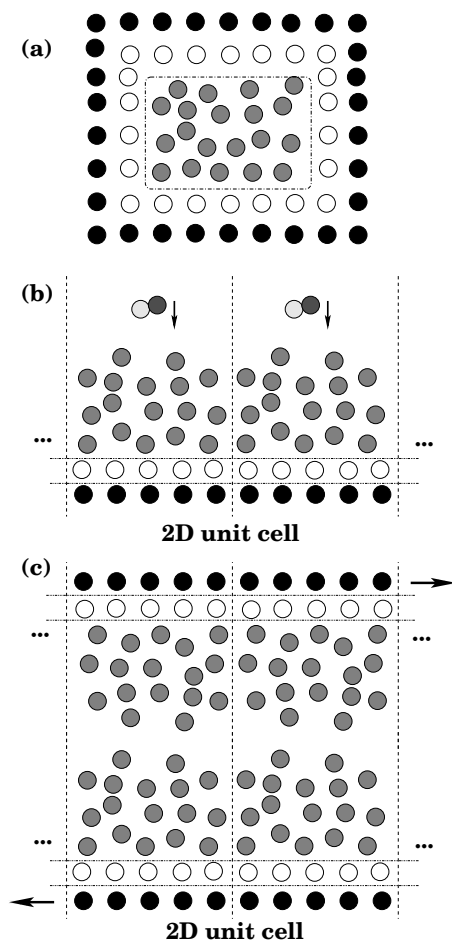


Figure 1: Schematic representation of the simulation systems treated with SBC: (a) a bulk system treated using a finite fragment; (b) a diatomic molecule is incident normally on the surface with periodic boundary conditions across the surface; (c) two surfaces slide upon each other, also with 2D periodic boundary conditions. Open circles indicate Langevin atoms, black circles correspond to fixed atoms (a,b) or atoms which move with predefined velocity in the case of sliding surfaces (c), while all other atoms (gray circles) are free to move according to ordinary Newtonian equations of motion. Note that in the case of the bulk, the Langevin and fixed atoms surround the internal region from all sides, while in the surface problems (b,c) these atoms are only placed at the outer edges of the system below (b,c) and above (c) the internal fragment of atoms.

surface is considered using the SBC and the Nosé thermostats and temperature distributions are compared. Section 4 is devoted to MD simulations of the friction caused by sliding two self-assembled monolayers of alkoxy silane molecules, chemisorbed on an amorphous silica surface, with respect to each other. Finally, brief conclusions are made in Section 5.

## 2 Implementation of Stochastic Boundary Conditions

In our MD simulations with the SBC we divide the system into three regions [63] as schematically shown in Fig. 1 for both cases studied here: the irradiation problem when a molecule projectile hits a Si(001) surface (b), and the tribology problem (c) when two surfaces covered by adsorbed molecules slide with respect to each other. In both cases periodic boundary conditions (PBC) across the surface are applied. In all these cases three regions of atoms are chosen: atoms coloured black in the Figure are either fixed (b) or rigidly move with a constant velocity in the case of sliding (c), as indicated. The internal atoms in the systems (gray) move freely according to Newtonian dynamics. Finally, there is a buffer region of Langevin atoms between the internal and fixed atoms which are coloured white. The Langevin atoms participate in MD simulations, however, on top of the forces due to other atoms in the system they experience also friction and random forces, as described above.

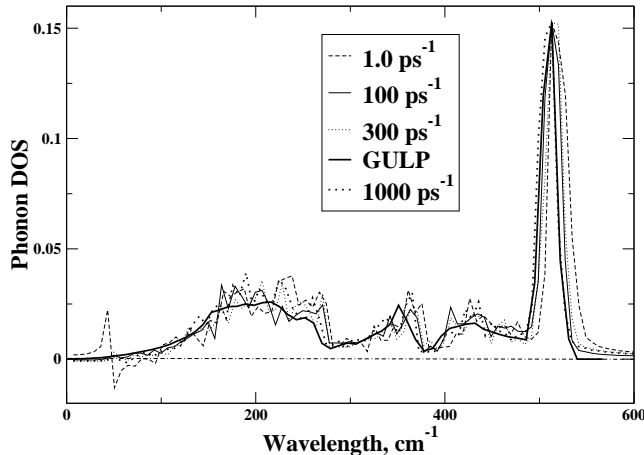


Figure 2: Calculated phonon DOS from lattice dynamics (solid curve) and from an isolated cluster of 4096 atoms treated with the SBC. In the latter case different values of the friction constant were used as indicated.

In the radiation problem, we are interested in applying the SBC specifically to the Si(001) surface. In order to use the SBC, it is necessary to assign a friction constant to every degree of freedom associated with the silicon Langevin atoms. In theory, the friction constants  $\gamma_i$  may be different for non-equivalent atoms; in practice, however, the same constant  $\gamma$  is assigned to all three Cartesian components of all Langevin atoms.

In order to obtain the appropriate value for the friction constant, we, following the method of [41, 68], first considered a Si bulk crystal using the Tersoff force field [69]. Using the GULP code [70], we calculated the phonon density of states (DOS) of the Si bulk crystal from the lattice dynamics calculations; 5342  $\mathbf{k}$ -points in the irreducible Brillouin zone were used. This DOS is to be considered as a reference when selecting the value of the friction constant. Then, we considered an isolated silicon 16x16x16 cluster in the form of a cube containing 4096 atoms which was chosen to model the silicon bulk. In this cluster, the external two layers were fixed and atoms in a single internal layer next to the fixed ones were treated as Langevin atoms. Note that in these simulations fixed and Langevin atoms were at all six faces of the system cube since we were simulating the silicon bulk, see Fig. 1(a). The same Tersoff force field, as implemented in the Sci-Fi code [65], was used. Using this cluster, we performed MD runs with SBC at 300K for several values of the friction constant: 1, 10, 50, 100, 300 and 1000  $\text{ps}^{-1}$ . In all these simulations, the system was first equilibrated for 50 ps, and then the run was restarted for another 10 ps with the timestep of 1 fs (see below). From the Fourier transform of the atomic-diagonal velocity autocorrelation functions obtained using the last 10 ps of the MD runs, we calculated the phonon DOS in each case. The calculated DOS for a selected values of  $\gamma$  are compared with the reference DOS obtained directly from the lattice dynamics using the GULP code in Fig. 2. We find that if the  $\gamma$  is too small, it results in artificial wiggles at small wavelengths. Very large values of  $\gamma$  lead to unnecessary fluctuations of the DOS in the intermediate region. The values of the friction constant between 100 and 300  $\text{ps}^{-1}$  do not have noticeable effect on the phonon DOS. In all our calculations described below the value of  $\gamma = 100 \text{ ps}^{-1}$  was chosen.

When performing *ab initio* DFT based simulations, the same value for the friction constant can be used. This is because the Tersoff force field was fitted to crystal properties associated with small atomic displacements, so that the lattice dynamics of the bulk silicon crystal observed via the DFT method should be reproduced reasonably well.

It is instructive at this point to demonstrate also the ability of the SBC to serve as a canonical thermostat. To this end, we considered the same isolated silicon 16x16x16 cluster as above using the friction constant of 100  $\text{ps}^{-1}$  for the Langevin atoms. In Fig. 3 the temperature in the cluster during the equilibration time of around 50 ps is shown for two values of the time step and the target temperature of 750 K. One can clearly see that, indeed, the SBC works perfectly as a thermostat, in agreement with other studies, and also that the equilibration evolution practically does not change if the time step is reduced to 0.5 fs. We also checked that the simulations with longer timestep of 2 fs (not shown) results in somewhat distorted behaviour for the temperature. Therefore, the timestep of 1.0 fs was chosen for all our MD simulations which are reported here.

In the sliding calculations (Section 4), we considered self-assembled monolayers (SAMs) of methyl-terminated hydrocarbon alkoxy silane ( $-\text{O}-(\text{CH}_2)_{10}\text{CH}_3$ ) molecules attached to two amorphous  $\text{SiO}_2$  surfaces which move in the opposite directions with a constant velocity as schematically shown in Fig. 1(c). To model the energy transfer through the upper and lower faces of the simulation system into the corresponding bulk of the upper and lower crystals, respectively, we introduce the upper and the lower layers of Langevin atoms. These are followed on

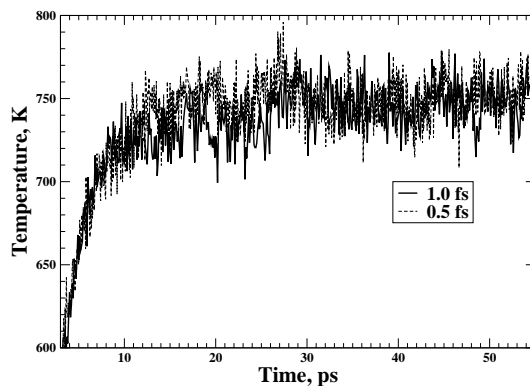


Figure 3: Temperature fluctuations in the 16x16x16 isolated cluster with the SBC (see text) during the equilibration stage MD for two time steps of 0.5 fs (broken curve) and 1.0 fs (solid curve). The target temperature in both cases is 750 K and the friction constant  $\gamma = 100 \text{ ps}^{-1}$ .

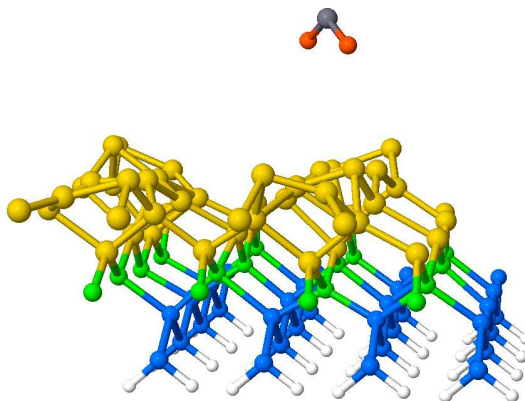


Figure 4: Simulation cell used in *ab initio* DFT calculations of the  $\text{CaF}_2$  molecule projectile on the Si(001) surface. The colour scheme corresponds to different species and functionality of various atoms (see text).

the outside by fixed atoms (coloured black) which are designed to provide the correct potential for the Langevin atoms, similarly to the previously considered cases. The sliding of the two surfaces with respect to each other is accomplished by rigidly moving these fixed atoms in the opposite directions as indicated in the Figure. In principle, in order to describe correctly the energy transfer through the boundary region, values of the friction constants  $\gamma_{Si}$  and  $\gamma_O$  for the two species (Si and O) need to be obtained. It may seem that this can be done, as for the Si system above, by comparing velocity autocorrelation functions (or their averages over various groups of atoms) calculated for the silica bulk with PBC and using SBC, with a relatively large finite fragment of the crystal in the latter case. However, the situation is complicated by the fact that we deal here with an amorphous silica, so it is not entirely clear whether the friction constants obtained for the silica bulk would be appropriate in this case. Since in the present study we are mostly interested in the qualitative aspects of thermostating, we decided to use the same friction constant for both species of  $\gamma = 10 \text{ ps}^{-1}$ . This value ensures relatively fast initial equilibration of the whole system via the Langevin thermostat applied to *all* atoms of the static system, i.e. when the two surfaces do not move with respect to each other.

### 3 Irradiation of the Si(001) surface with a $\text{CaF}_2$ molecule

Irradiation of the Si(001) surface with  $\text{CaF}_2$  molecules at around 1020 K leads to the formation of a wetting layer, on which further evaporation results in the growth of 1D nanowires [71]. The atomistic mechanism of the wetting layer formation is not understood, however, there are indications [72] that at the initial stages of the reaction between the descending  $\text{CaF}_2$  molecules and the Si(001) surface an etching process takes place with F atoms leaving the surface with Si atoms. A comprehensive investigation of this process goes far beyond the scope of this paper which is devoted to understanding of the issues related to using the correct thermostat in MD simulations. Therefore



we shall only consider several MD simulations directly related to this process in which a single  $\text{CaF}_2$  molecule is deposited on the Si(001) surface. Specifically, we shall compare the results of the dynamics obtained using two different thermostats: one simulation is done by means of the equilibrium Nosé-Hoover thermostat, and another using the SBC. In both cases the surface had a temperature of 1300K. The choice of the mass for the Nosé-Hoover thermostat, from the physical point of view at least, is somewhat arbitrary. In this study, we have used the value of  $100 \text{ fs}^2\text{Ry}$  for this mass.

We used the *ab initio* DFT SIESTA code [67] employing periodic boundary conditions, method of pseudopotentials and a localised basis set. The MD calculations were performed using Perdew-Burke-Ernzerhof GGA functional, double- $\xi$  basis with polarization orbitals and cutoff parameter for the grid set to 150 Ry. The following electrons were included explicitly in the calculations:  $\text{Si}(3s^23p^2)$ ,  $\text{Ca}(3s^23p^64s^2)$  and  $\text{F}(2s^22p^5)$ .

The simulation cell is shown in Fig. 4. The surface slab consists of 6 layers of Si atoms with the top layer containing two rows of Si dimers with 4 dimers in each. The bottom layer is terminated with hydrogen atoms (shown white); the bottom two layers of Si atoms (blue) and the hydrogen atoms are fixed, all other layers of Si atoms (green and yellow) are free to move. When using the SBC, the layer next to the fixed layers (coloured green) was considered as stochastic (i.e. Langevin) with the same friction constant as in our classical MD simulations. In simulations based on the Nosé-Hoover thermostatting, both green and yellow Si atoms and the molecule were thermostated.

To equilibrate the surface, we first run classical MD simulations using the Sci-Fi code until the temperature of the system started to fluctuate around the target temperature. The obtained atomic positions and velocities were then used as an input for the SIESTA code, which was run for additional 500 fs. After that, a  $\text{CaF}_2$  molecule, thermalised at temperature of 1300 K, was given a vertical velocity of  $0.05 \text{ \AA}/\text{fs}$  towards the surface, and then an MD simulation was run for an additional 1.5 ps.

The temperatures of the molecule and of the movable atoms of the surface for the two thermostats during the course of the simulations are shown in Fig. 5, while the corresponding averaged temperature distributions of the molecule and the surface are plotted in Figs. 6 and 7, respectively. Several interesting observations can be made by comparing the results of the simulations obtained with the two different thermostats. Firstly, we note that the temperature distribution of the molecule obtained with SBC is considerably wider than that obtained with the equilibrium thermostat. The temperature distributions of the surface atoms simulated with the two thermostats, on the other hand, are similar in shape; however, the stochastic thermostatting leads to generally hotter surface atoms. Secondly, the temperature of the  $\text{CaF}_2$  molecule decays with time much faster in the Nosé-Hoover simulations than with the SBC; some oscillatory behaviour of the temperature of the molecule with time in the former case is also visible. The SBC simulations suggest that the molecule dissipates its energy to the surface gradually, bit by bit. Even after 1 ps, the molecule remains hot in SBC calculations, giving out its energy to the surface much slower than one would expect when using the equilibrium thermostatting.

These differences are due to different mechanism of temperature control in the two thermostats. The Nosé-Hoover thermostat tries to cool down the whole system at the same time without taking into account the fact that the energy of the hot  $\text{CaF}_2$  molecule is being transferred to the surface gradually, and that it requires some time for that extra energy to dissipate through the surface into the silicon bulk. As the result, the time dependence of the temperature in the surface decays much faster than in the SBC calculations, and also the surface atoms in the calculation based on the equilibrium thermostatting are colder than they should be according to the SBC based calculations. In this respect, the SBC calculations deliver the correct physical picture: since the energy is being transferred from the molecule to the surface and it takes a finite time to dissipate this energy into the bulk, the surface would appear somewhat hotter over time. The temperature distribution and its time dependence obtained using the Nosé-Hoover thermostat are inconsistent with this picture.

## 4 Sliding simulations

In this Section we discuss the simulations of the shear response of methyl-terminated hydrocarbon alkoxy silane SAMs ( $-\text{O}-(\text{CH}_2)_{10}\text{CH}_3$ ) adsorbed on the silica surface. The tribological properties of these SAMs have been studied previously in [73]. All of the simulations were carried out using the LAMMPS molecular dynamics code [66]. The SAMs and silica substrate are modeled using the OPLS force field [74]. The SHAKE algorithm was used to constrain all hydrogen-containing bonds in the system [75]. A 1 fs time step was used with the velocity Verlet integrator. The van der Waals interactions were cut off at 1.0 nm, and a slab version of the PPPM algorithm was used to compute the long-range Coulomb interactions [76].

The initial configuration consisted of the alkoxy silane molecules chemisorbed on an amorphous silica substrate. The silica substrates were generated by quenching a liquid silicon oxide sample to a low temperature. Then

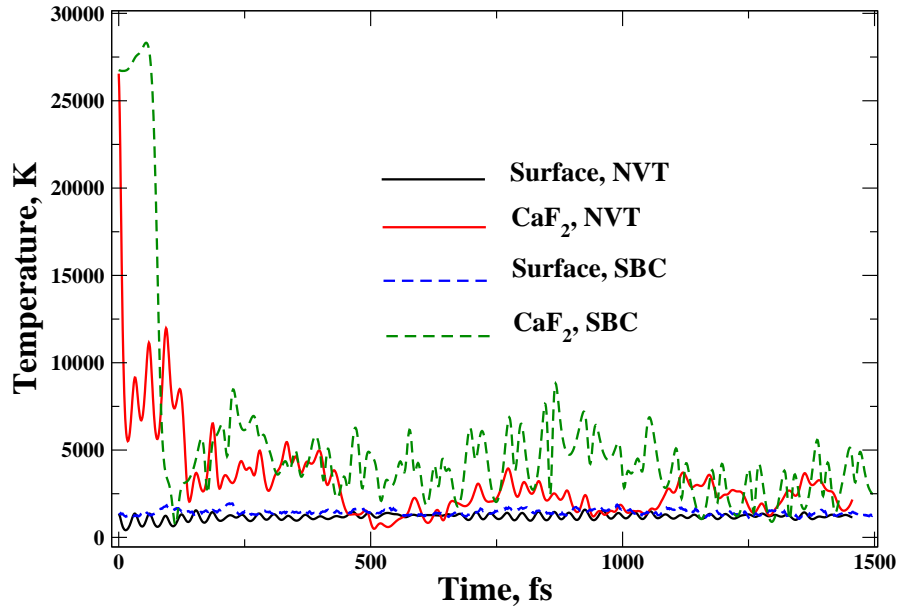


Figure 5: Time evolution of the temperature of the movable surface atoms and of the molecule during the MD simulations of the  $\text{CaF}_2/\text{Si}(001)$  system obtained using the NVT Nosé-Hoover and SBC thermostats.

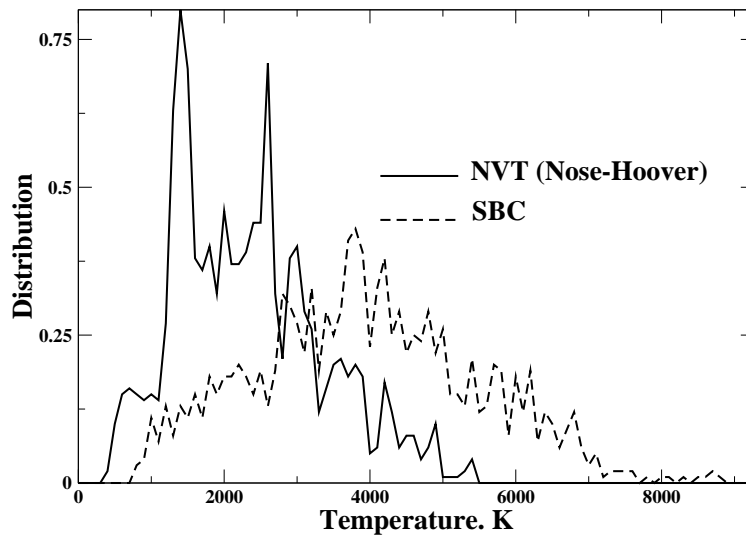


Figure 6: Computed average temperature distributions of the  $\text{CaF}_2$  molecule in the MD simulations of the  $\text{CaF}_2/\text{Si}(001)$  system performed using NVT (Nosé-Hoover) and SBC thermostats.

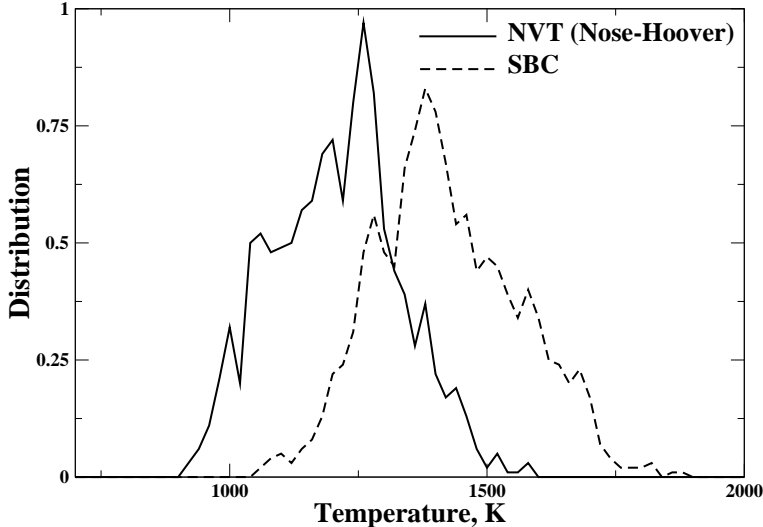


Figure 7: Computed average temperature distributions of the movable atoms of the Si(001) surface in the MD simulations of the  $\text{CaF}_2/\text{Si}(001)$  system performed using NVT (Nosé-Hoover) and SBC thermostats.

two interfaces were generated by cleaving the system in the  $z$ -dimension perpendicular to the surface. These substrates are subsequently annealed until the substrate has a silanol density that is consistent with that observed experimentally ( $\approx 4.6 \text{ OH}/\text{nm}^2$ ) [77]. A full description of the algorithm can be found in [78, 79, 80].

The alkoxy-silane molecules were added to the substrate to achieve a surface density corresponding to an area of  $0.25 \text{ nm}^2$  per chain by removing randomly chosen silanol groups from the silica surface and placing the alkoxy-silane chain in its place. The overall dimensions of the SAMs in the unit cell are  $55.2 \text{ \AA} \times 55.8 \text{ \AA} \times 30 \text{ \AA}$ . The SAM constructed in this way and the silica were thermalized for 50 ps using the Langevin thermostat applied to all atoms of the system except of the frozen atoms at the very bottom of the substrate. Then, the same substrate and the SAM were used for both the top and bottom interfaces.

Initially, the two SAM coated surfaces were placed such that the terminal carbons of the two opposing SAMs were separated by approximately  $15 \text{ \AA}$ . To apply a load during the shear, the two surfaces were driven towards each other at a rate of 2 m/s (“compressed”). Although these compression rates are high compared to experiment, the previous work demonstrated that for similar systems the velocity does not have a strong effect on the contact force [78]. From these compression runs, three different equilibrated spacings between the SAMs were obtained which we shall refer to as systems A (largest separation), B (intermediate separation) and C (smallest separation). The configurations for the system at the three different separations were used in constant volume simulations from which all of the data presented in the following were generated. Fig. 8 shows a snapshot of system B.

The shear is applied by moving the two silica substrates in opposite directions. Most of the results reported here were obtained at the velocity of 1 m/s corresponding to the relative shear velocity of 2 m/s. Each system is sheared for 5 ns and the data are averaged over the entire course of the simulation.

We have applied several different thermostating schemes to this system. Figure 8 (b) shows a colour-coded snapshot of the various regions defined in the system in order to apply the different thermostats. In one set of simulations we used a traditional equilibrium NVT Langevin thermostat applied to most of the atoms (blue and red) with a friction coefficient of  $10 \text{ ps}^{-1}$  to maintain a temperature of 300 K; the rest of the atoms (black) were frozen and used to apply the shear velocity and the loads. In another set of simulations the friction and random forces are applied to the same atoms, but only in the direction perpendicular to the shear and compression in order to minimize their direct effect on the dynamics of the system [81]; this will be referred to as NVT (Langevin) 1D, whereas the former method - as NVT (Langevin) 3D. These two schemes are compared with the SBC thermostating scheme of Fig. 1 (c) in which the same atoms were frozen and used to apply the shear and loads (black atoms); however, the nearest and next nearest neighbors of these atoms were considered as Langevin atoms (red) to which the random and friction forces are applied in *all three* directions; finally the bulk of the system is not thermostatted in this case (blue atoms), i.e. their dynamics are Newtonian.

We have calculated the friction force and applied load values by averaging each force during the course of the shear simulations. From these data, we determine a microscopic coefficient of friction  $\mu$  by considering that the friction depends upon both the load and the area, i.e.  $F = \alpha A + \mu F_{\perp}$ , where  $F$  is the friction force,  $\alpha$  is a constant,

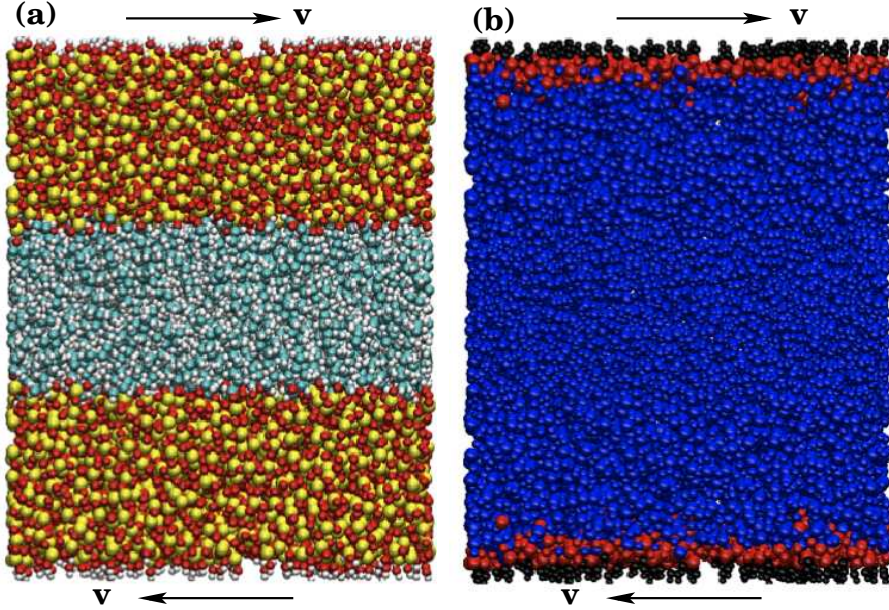


Figure 8: (a) Snapshot of the simulation system B before shear. The different colours represent the different atomic species in the system: oxygen (red), silicon (yellow), hydrogen (grey), and carbon (teal). (b) Snapshot of same system with different colours identifying the three different regions used in two different thermostating schemes: (i) traditional equilibrium NVT thermostat (Langevin in this case): frozen atoms (black), Langevin atoms (red and blue); (ii) SBC thermostat: frozen atoms (black), Langevin atoms (red), atoms not thermostated (blue). The shear is applied by assigning a velocity  $v$  to a layer of frozen silica atoms (black) on the outer edges of the silica substrates.

$A$  is the contact area and  $F_{\perp}$  is the applied load. Therefore the slope of the friction force *versus* applied load gives  $\mu$ . The typically measured "macroscopic" coefficient of friction encompasses a number of issues (i.e. microscopic roughness and asperity contact) that we do not treat in these parallel slab geometry. Therefore the microscopic  $\mu$  calculated from these simulations is a necessary input to calculate the macroscopic  $\mu$ .

The dependence of the lateral friction force on the applied load for the shear velocity of 2 m/s is shown in Fig. 9. Although one can notice some small differences in the calculated load and friction forces, for all loads considered here the value of  $\mu$  is nearly the same within error for each thermostat (between 0.17 and 0.19).

The dependence on the thermostating on shear velocity can be seen in Fig. 10 where the average friction force is shown calculated for system B for three different relative shear velocities of 2, 20 and 200 m/s. The friction force calculated with the NVT (Langevin) 3D thermostat deviates noticeably from the results of the SBC based calculations at the highest velocity of 200 m/s we considered. At the same time, we also see that if the friction and random forces are only applied in the direction perpendicular to the shear and compression (the NVT (Langevin) 1D thermostat), the results of the friction versus shear velocity are close to those obtained in the SBC based calculations, even at the highest shear velocity.

To understand the reasons behind these behaviours, we have also looked at the temperature distribution across the whole system (slab) in the direction perpendicular to the surface. The temperature profile establishes itself very quickly after the surfaces start to move and after that does not change appreciably with time in our simulations, i.e. what we observe is a steady-state distribution of the temperature. We also found very small dependence of the temperature profile for either of the thermostats on the applied load (i.e. the SAMs separation). However, we find that the temperature profile does depend on the relative shear velocity. In Fig. 11 the temperature profiles calculated for system B at 300K and three shear velocities are shown. Apart from the SBC calculations, only data corresponding to the NVT (Langevin) 1D thermostat are shown as no difference has been found in the calculations with the NVT (Langevin) 3D thermostat. One can clearly see that the profiles calculated with the two thermostats are similar in shape with a noticeable dip in the temperature in the middle of the simulated system, i.e. in the region where the molecules of the two SAMs interpenetrate. Moreover, at shear rates of 2 m/s and 20 m/s the temperature distributions are practically the same. The only considerable difference is that the SBC based simulations predict the temperature of the system to be considerably higher at higher shear velocities, which is the result one would intuitively expect; of course, no such behaviour is predicted by either of the NVT based simulations, when the

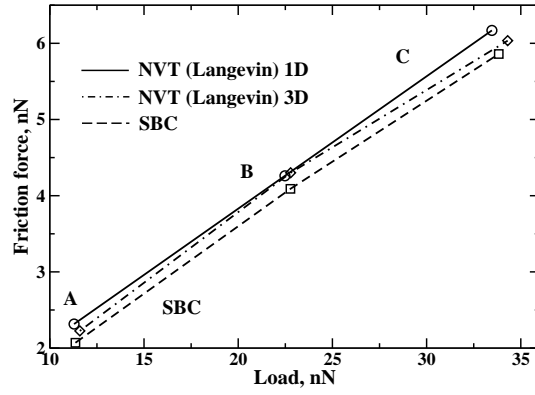


Figure 9: Average friction force as a function of the applied load calculated using both variants of the NVT (Langevin) scheme and the SBC thermostating for the systems A, B and C. The two surfaces were sheared with respect to each other with the smallest relative velocity of 2 m/s.

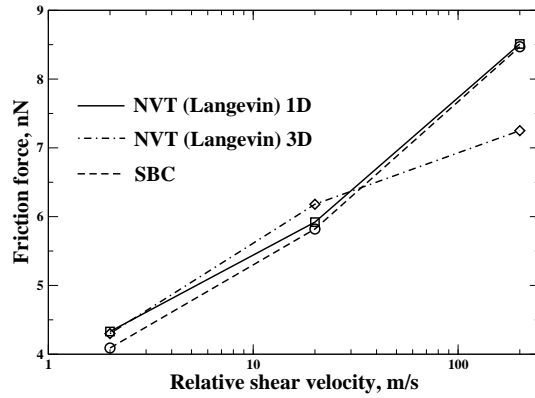


Figure 10: Average friction force as a function of the relative shear velocity calculated for system B using three thermostating methods: two different equilibrium approaches (1D and 3D Langevin, see text) and SBC.

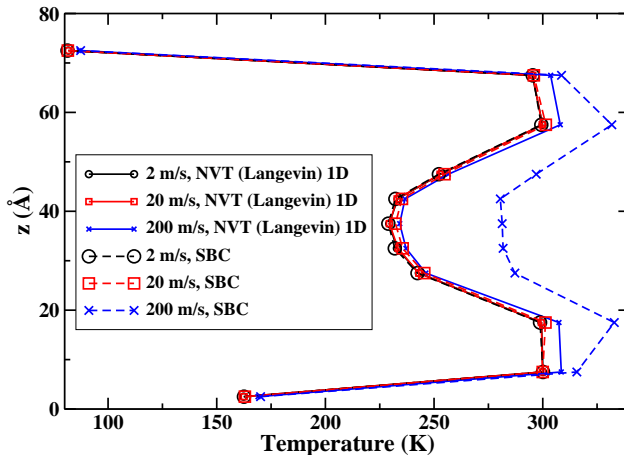


Figure 11: Steady-state temperature profile across the simulated system B in the direction perpendicular to the surfaces for three different relative shear velocities  $v$ , calculated using SBC (broken lines) and equilibrium NVT (Langevin) 1D (solid lines) thermostats. All simulations were done at 300K.

system is forced to stay at 300K irrespective of the velocity.

Since the temperature profiles for the two thermostats do not noticeably differ for the smallest velocity of 2 m/s, the data in Fig. 9 can be easily understood. Indeed, at this relatively small shear velocity the system can be considered as in quasi-equilibrium, i.e. the two surfaces move with respect to each other slower than is required to establish thermodynamic equilibrium in the system. At the highest shear velocity, however, the friction calculated with SBC is much higher than using the NVT (Langevin) 3D thermostating because the system in the middle of the slab (which is mainly responsible for the friction) is much cooler in the latter case, see Fig. 11.

The fact that the friction forces calculated within the SBC and the NVT (Langevin) 1D thermostating schemes are similar for all considered shear velocities is somewhat puzzling, however. Indeed, in SBC based simulations the friction and random forces are only applied to the atoms which are close to the system boundary and hence are responsible for the energy exchange with the environment; atoms of the methyl-terminated hydrocarbon alkoxyisilane molecules experience only “physical” forces due to other atoms in the system. On the other hand, in the NVT (Langevin) 1D simulations, the artificial friction and random forces are applied in a single direction to *all atoms* of the slab, including the central region where the molecules interpenetrate. Both NVT based simulations show identical temperature profiles; specifically, at  $v = 200$  m/s the system is much cooler in the middle region in both simulations than when the SBC is applied. Why then the friction force does come out nearly the same in the NVT (Langevin) 1D scheme as in the SBC calculations in which the system is much hotter in the middle? We believe that the reason lies in the way the Langevin dynamics is conducted in the NVT (Langevin) 1D based simulations: here the friction and random forces are not applied in the directions along the shear and of the load, i.e. the atomic forces in these directions are less affected; as the result, these simulations result in nearly correct friction and load forces due to cancellation of errors.

## 5 Conclusions

In this paper we have discussed the question of temperature control in MD simulations. If equilibrium thermostats, which sample the canonical distribution of the system, are perfectly applicable to equilibrium situations (e.g. calculating the kinetic coefficients, free energies or autocorrelation functions), we argue that these are not applicable to non-equilibrium problems in which some energy is given (taken) to (from) the system, as this energy will then dissipate (will be obtained) to (from) the environment, the latter is not represented explicitly in the simulation model. Although it is commonplace in the literature that equilibrium thermostating is used for genuinely non-equilibrium processes such as e.g. chemisorption, tribology, irradiation and fracture propagation, to name just a few, and in many instances, at least qualitatively, the results may be still physically meaningful, it is shown in this paper that in some cases an equilibrium thermostating may lead to wrong temperature distribution throughout the system, severely affected particles trajectories and, as a result of these, wrong physical conclusions.

The MD simulations of the  $\text{CaF}_2/\text{Si}(001)$  system performed employing an equilibrium thermostating demonstrated that the molecule cools down too quickly during the impact on the surface; depending on the parameters

used in the thermostatting, some artificial oscillations of the molecule temperature can also be observed. The surface atoms on average also lose their kinetic energy much too quickly than expected. In the sliding problem considered here using equilibrium thermostatting methods, we observe the temperature distribution being too low across the slab at very high shear velocities (200 m/s). This results in noticeably smaller values of the calculated friction force, unless the thermostat is employed such that the friction and random forces of the Langevin dynamics are only applied in the single direction perpendicular to the shear and load directions.

We should expect qualitatively inappropriate behaviours in other cases as well. Consider, for instance, an irradiation process when a particle with a significant kinetic energy is incident on a crystal surface kept at some temperature  $T$ . Even during the initial stages of the impact when the projectile still possesses a significant kinetic energy, which is much larger than the characteristic energy required to create a defect in a solid (several eV), i.e. during the ballistic part of the track, application of the correct thermostat may be important for understanding main processes which happen during the impact: using an inappropriate thermostat will affect significantly the time during which the projectile dissipates most of its energy and, in addition, the track structure may be qualitatively incorrect (e.g. the size of the affected area along the track will be underestimated). When the projectile is sufficiently slowed down, such that its energy becomes comparable with the characteristic defect formation energies, then using the correct thermostat becomes even more essential. This is because the process of defect creation in the track is an activation process which requires some time, and if an equilibrium thermostat is used which yields artificially fast cooling of the system, the time dependence of the dissipation process will be significantly affected. For instance, if the projectile loses its energy too quickly into the environment, then one may expect very few activation processes to happen and the track may be thin and with small concentration of defects. If this is not the case and the track remains hot for some considerable time (which is determined by the actual interatomic interactions in the solid), then one may expect formation of more defects and a healing processes to take place.

What is then the appropriate thermostat to use for doing MD simulations of non-equilibrium processes? We give several arguments in favour of the SBC which is a stochastic thermostat with only border atoms experiencing additional random and friction forces to control the flow of energy through the system border. The SBC follows from the exact description based on the GLE under the assumption of short-range interactions between atoms. GLE can be applied to any process, including non-equilibrium ones, and hence SBC, as a simplified version of it, should be perfectly applicable to treating truly non-equilibrium processes. The SBC thermostatting is based on a physically appealing intuitive idea that only border atoms should be affected by thermostatting since only these atoms “feel” the presence of the environment kept at a constant temperature; internal atoms of the simulated system should only experience “physical” forces due to surrounding atoms. In addition, the SBC is easy to implement because of its simplicity. At the same time, in spite of the approximations made, this method guarantees appropriate equilibrium NVT thermostatting, since in equilibrium any system would arrive at the correct canonical distribution with the desired temperature [63]. This was also demonstrated in some of the example systems considered in this paper.

The SBC also solves some technical issues. Indeed, when performing an MD simulation of a slab system, one has to fix bottom atoms of the slab to mimic the bulk not represented explicitly in the model. Because of these fixed atoms, free atoms in the next layer would be partially frustrated in their movement. As a result, even in equilibrium calculations these atoms on average would have lower temperature than atoms of the upper layers, i.e. there will be some artificial gradient of the temperature in the slab in the direction perpendicular to the surface. The SBC thermostat handles this problem in a very natural way by placing stochastic atoms as a buffer between the freely moving and fixed atoms in the slab, resulting in a much more realistic distribution of the temperature in the slab at equilibrium. This point becomes especially important in *ab initio* MD when one cannot afford thick slabs.

We note that the point of selecting the correct approach in dealing with non-equilibrium processes is not exclusively the MD problem. For instance, one can still find in the literature (see e.g. [82]) that non-equilibrium dynamics is considered using equilibrium canonical Monte Carlo (MC) [83], although applying Kinetic MC (KMC) instead [84, 45] would be physically more appropriate. After all, MC uses only total energies, while the KMC employs transition rates based on energy *barriers*.

Concluding, we discussed in this paper what must be an appropriate thermostat to be used for MD simulations of non-equilibrium processes, and argued that the method of choice is the Langevin thermostat applied to the border atoms only, the so-called Stochastic Boundary Conditions. This method has a triple benefit of being derived from the rigorous formulation based on the GLE, it arrives at the correct canonical distribution when the system reaches equilibrium and is very easy to implement. We hope that this study will stimulate further discussion concerning appropriate ways of performing MD simulations of non-equilibrium processes.

## Acknowledgement

NR and DT would like to acknowledge the financial support from EU PICO-inide project FP6-15847.

## References

- [1] M. P. Allen and D. J. Tildesley, *Computer simulation of liquids* (Clarendon Press, Oxford, 2002).
- [2] H. Berendsen, J. Postma, W. Vangunsteren, A. Dinola, and J. Haak, *J. Chem. Phys.* **81**, 3684 (1984).
- [3] H. C. Andersen, *J. Chem. Phys.* **72**, 2384 (1980).
- [4] S. Nose, *Mol. Phys.* **52**, 255 (1984).
- [5] S. Nose, *J. Chem. Phys.* **81**, 511 (1984).
- [6] W. Hoover, *Phys. Rev. A* **31**, 1695 (1985).
- [7] T. Schneider and E. Stoll, *Phys. Rev. A* **17**, 1302 (1978).
- [8] G. Bussi and M. Parinello, *Phys. Rev. E* **75**, 056707 (2007).
- [9] G. Bussi, D. Donaldo, and M. Parinello, *J. Chem. Phys.* **126**, 014101 (2007).
- [10] S. M. Kast, N. Kai, H.-J. Baer, and J. Brickmann, *J. Chem. Phys.* **100**, 566 (1994).
- [11] D. N. Payton, M. Rich, and W. M. Visscher, *Phys. Rev.* **160**, 706 (1967).
- [12] R. Tehver, F. Toigo, J. Koplik, and J. R. Banavar, *Phys. Rev. E* **57**, R17 (1998).
- [13] P. L. Garrido, P. I. Hurtado, and B. Nadrowski, *Phys. Rev. Lett.* **86**, 5486 (2001).
- [14] S. Lepri, R. Livi, and A. Politi, *Physics Reports* **377**, 1 (2003).
- [15] P. T. Mikulski, G. M. Gao, G. an Chateaufneuf, and J. A. Harrison, *J. Chem. Phys.* **122**, 024701 (2005).
- [16] I. Szlufarska, R. K. Kalia, A. Nakaro, and P. Vashishta, *J. Appl. Phys.* **102**, 023509 (2007).
- [17] T. Zykova-Timan, D. Ceresoli, and E. Tosatti, *Nature Mater.* **6**, 230 (2007).
- [18] U. Landman, W. D. Luedtke, and J. Gao, *Langmuir* **12**, 4514 (1996).
- [19] J. Gao, W. D. Luedtke, and U. Landman, *Science* **270**, 605 (1995).
- [20] J. Gao, W. D. Luedtke, D. Gourdon, M. Ruths, J. N. Israelachvili, and U. Landman, *J. Phys. Chem. B* **108**, 3410 (2004).
- [21] J. Gao, W. D. Luedtke, and U. Landman, *J. Phys. Chem. B* **102**, 5033 (1998).
- [22] P. T. Mikulski, L. A. Herman, and J. A. Harrison, *Langmuir* **21**, 12197 (2005).
- [23] G. T. Gao, P. T. Mikulski, and H. J. A., *J. Am. Chem. Soc.* **124**, 7202 (2002).
- [24] I. Jang *et al.*, *J. Appl. Phys.* **102**, 123509 (2007).
- [25] P. R. Barry *et al.*, *J. Phys.: Condens. Matter* **21**, 144201 (2009).
- [26] S. Heo and S. B. Sinnott, *J. Appl. Phys.* **102**, 064307 (2007).
- [27] W.-D. Hsu, S. Tepavcevic, L. Hanley, and S. B. Sinott, *J. Phys. Chem. C* **111**, 4199 (2007).
- [28] Y. Hu and S. Sinnott, *J. Comp. Phys.* **200**, 251 (2004).
- [29] P. Kluth *et al.*, *Physical Review Letters* **101**, 175503 (2008).
- [30] K. Meinander and K. Nordlund, *Phys. Rev. B* **79**, 045411 (2009).



- [31] K. Nordlund *et al.*, Phys. Rev. B **57**, 7556 (1998).
- [32] Y. Hu *et al.*, J. Chem. Phys. **116**, 6738 (2002).
- [33] I. Jang and S. B. Sinnott, J. Phys. Chem. B **108**, 18993 (2004).
- [34] T. Aoki and J. Matsuo, Applied Surface Science **252**, 6466 (2006).
- [35] J. R. Kermode *et al.*, Nature, **455**, 1224 (2008).
- [36] A. De Vita, private communication, about thermostat used, 2009.
- [37] D. West and S. K. Estreicher, Phys. Rev. Lett. **96**, 115504 (2006).
- [38] H. A. Scheraga, M. Khalili, and A. Liwo, Annu. Rev. Phys. Chem. **58**, 57 (2007).
- [39] M. T. Gallo *et al.*, Mol. Simul. **35**, 349 (2009).
- [40] T. Trevethan and L. Kantorovich, Phys. Rev. B **70**, 115411 (2004).
- [41] T. Trevethan and L. Kantorovich, Nanotechnology **15**, S44 (2004).
- [42] B. J. Garrison, P. B. S. Kodali, and D. Srivastava, Chem. Rev. **96**, 1327 (1996).
- [43] C. L. Brooks III and M. Karplus, J. Chem. Phys. **79**, 6312 (1983).
- [44] M. Berkowitz and J. McCammon, Chem. Phys. Lett. **90**, 215 (1982).
- [45] L. Kantorovich, Phys. Rev. B **75**, 064305 (2007).
- [46] H. Mori, Prog. Theor. Phys. **33**, 423 (1965).
- [47] R. Zwanzig, J. Stat. Phys. **9**, 215 (1973).
- [48] R. Zwanzig, *Nonequilibrium statistical mechanics* (Oxford Univ. Press, 2001).
- [49] S. Adelman and J. Doll, J. Chem. Phys. **64**, 2375 (1976).
- [50] S. A. Adelman, J. Chem. Phys. **71**, 4471 (1979).
- [51] J. C. Tully, J. Chem. Phys. **73**, 1975 (1980).
- [52] E. Cortes, B. J. West, and K. Lindenberg, J. Chem. Phys. **82**, 2708 (1985).
- [53] D. J. Diestler and M. E. Riley, J. Chem. Phys. **83**, 3584 (1985).
- [54] R. Tsekov and E. Ruckenstein, J. Chem. Phys. **100**, 1450 (1994).
- [55] R. Tsekov and E. Ruckenstein, J. Chem. Phys. **101**, 7844 (1994).
- [56] M. Moseler, J. Nordiek, and H. Haberland, Phys. Rev. B **56**, 15439 (1997).
- [57] E. Hernandez, J. Chem. Phys. **115**, 10282 (2001).
- [58] G. J. Wagner, E. G. Karpov, and W. K. Liu, Comput. Methods Appl. Mech. Engrg. **193**, 1579 (2004).
- [59] E. G. Karpov, G. J. Wagner, and W. K. Liu, Int. J. Numer. Mech. Engrg. **62**, 1250 (2005).
- [60] A. V. Popov, J. Melvin, and R. Hernandez, J. Phys. Chem. **110**, 1635 (2006).
- [61] E. G. Karpov, H. S. Park, and W. K. Liu, Int. J. Numer. Mech. Engrg. **70**, 351 (2007).
- [62] L. N. Kantorovich, Phys. Rev. B **78**, 094304 (2008).
- [63] L. N. Kantorovich and N. Rompotis, Phys. Rev. B **78**, 094305 (2008).
- [64] J.-S. Wang, Phys. Rev. Lett. **99**, 160601 (2007).

- [65] L. N. Kantorovich, T. Trevethan, J. Polesel-Maris, N. Martsinovich, and A. Foster, Sci-Fi code (Self-Consistent Image Force Interaction + virtual AFM machine), unpublished.
- [66] S. J. Plimpton, *J. Comp. Phys.* **117**, 1 (1995).
- [67] J. M. Soler *et al.*, *J. Phys.: Condens. Matter* **14**, 2745 (2002).
- [68] T. Trevethan and L. Kantorovich, *Phys. Rev. B* **70**, 115411 (2004).
- [69] J. Tersoff, *Phys. Rev. B* **38**, 9902 (1988).
- [70] J. Gale and A. Rohl, *Mol. Simul.* **29**, 291 (2003).
- [71] L. Pasquali *et al.*, *Phys. Rev. B* **72**, 045448 (2005).
- [72] N. S. Sokolov *et al.*, *Appl. Surf. Science* **234**, 480 (2004).
- [73] M. Chandross, C. D. Lorenz, M. J. Stevens, and G. S. Grest, *Langmuir* **24**, 1240 (2008).
- [74] W. J. Jorgensen, D. S. Maxwell, and J. Tirado-Rives, *J. Am. Chem. Soc.* **118**, 11225 (1996).
- [75] J. P. Ryckaert, G. Ciccotti, and H. J. C. Berendsen, *J. Comput. Phys.* **23**, 327 (1977).
- [76] P. S. Crozier, R. L. Rowley, and D. Henderson, *J. Chem. Phys.* **113**, 7513 (2001).
- [77] R. K. Iler, *The Chemistry of Silica* (Wiley: New York, 1979).
- [78] M. Chandross, E. B. Webb, M. J. Stevens, G. S. Grest, and S. H. Garofalini, *Phys. Rev. Lett.* **93**, 166103 (2004).
- [79] C. D. Lorenz, M. Chandross, G. S. Grest, M. J. Stevens, and E. B. Webb, *Langmuir* **21**, 11744 (2005).
- [80] C. D. Lorenz and A. Travesset, *Phys. Rev. E* **75**, 061202 (2007).
- [81] P. A. Thompson and M. O. Robbins, *Science* **250**, 792 (1990).
- [82] D. Kadau, A. Hucht, and D. E. Wolf, *Phys. Rev. Lett.* **101**, 137205 (2008).
- [83] D. Frenkel and B. Smith, *Understanding Molecular Simulation: From Algorithms to Applications* (Academic Press, San Diego, CA, 2002), .
- [84] A. F. Voter, *Radiation effects in solids* NATO Publishing unit Handbook of Material Modeling, Part A. Methods (Springer, NATO Publishing Unit, Dordrecht, The Netherlands, 2005), .